Design and implementation of DC-to-DC converter topology for current regulated lightning generator

Vincent Andraud, Rafael Sousa Martins, Clément Zaepffel, Romaric Landfried, Philippe Teste

Design and implementation of DC-to-DC converter topology for current regulated lightning generator

V Andraud[1], R Sousa Martins[1], C Zaepffel[1], R Landfried[2] and P Testé[2]

[1]DPHY, ONERA, Université Paris Saclay, F-91123 Palaiseau, France

[2]Laboratoire GeePs, CNRS UMR8507, Université Paris Saclay, CentraleSupélec, 91190 Gif-sur-Yvette, France

E-mail: rafael.sousa_martins@onera.fr

Abstract

When aircraft are impacted by lightning strikes, structural fuselage and components are stressed by electric and thermo-mechanical constraints, which impose a need for reliable experimental test benches to design accurate and enhanced lightning protections. The aim of this work is to investigate, design and compare different topologies of DC high-current generators in order to experimentally reproduce the continuous lightning current waveform component applied to produce an electric arc up to 1 meter long. An electrical model of a standard lightning C*-waveform for 1 m long arc is set, leading to an equivalent resistor varying from 4 to 8 Ω. This model enables a theoretical comparison between the DC/DC converters Buck and Buck-boost topologies to generate such a current-regulated waveform through a load using a capacitor bank and applying a minimum initial stored energy criterion. The experimental implementations of Buck and Buck-boost configurations are designed and tested. Optimizations about the accuracy of the current regulation through feedback loop and the respect of components operating electrical and power parameters are presented. In particular, the implementation of a snubber filter and a frequency control of the switching operations, which are mandatory elements in the operation of DC converters, are described to prevent the circuit from damaging initiated by transient overvoltage peaks. Both Buck and Buck-boost configurations are experimentally implemented to perform a standard C*waveform through a 4 Ω resistor and the Buck configuration proves ability to generate electric arcs up to 1.5 m respecting the standard aeronautic waveform of lightning.

I/ Introduction

A. Lightning on aircraft

Lightning strike is a phenomenon that cannot be undermined in the aeronautical industry since an aircraft is statistically stroke every 1000 to 10000 flight hours.[1,2] The new generation of aircrafts with outer skin and wings made of composite materials addresses new issues to the consideration of the direct effects of lightning. Whereas the aluminum material can endure the direct electric and thermo-mechanical damage provoked by a lightning strike without risks for the aircraft structure, carbon composite has lower coefficients of thermal and electrical diffusions causing that the damage from the impact zone is not supported by the overall structure. It is thus necessary to understand the physical mechanisms that are implied in this lightning direct strike phenomenon to aeronautical material and to develop and optimize lightning strike protections. There is a large bibliography about the modelling and the simulations of lightning arc interactions with aeronautical material.[3-7] As the lack of relevant experiments prevents from relying only on the existing simulation codes, lightning generators need to be designed and constructed to reproduce lightning tests in laboratory and to create experimental reference database for the physical parameters of the phenomenon.

In the context of protection of aeronautical equipment from lightning strikes, standards and recommendation of lightning current waveform has been settled to reproduce experimentally the direct effects of lightning over aircraft equipments.[8-9] The document introduces different waveform phases as non-superposed current waves that can be tested either successively or independently in order to separate the different kinds of structural damages induced by those different phases as depicted in Fig. 1. The objective of the generator developed in this paper is to accurately reproduce the C-waveform described in the ARP5412A recommendation document. The C-waveform is represented as a continuous square-shaped current of 200 to 800 A that is maintained during 250 to 1000 ms resulting in at least 200 C of charge transfer.

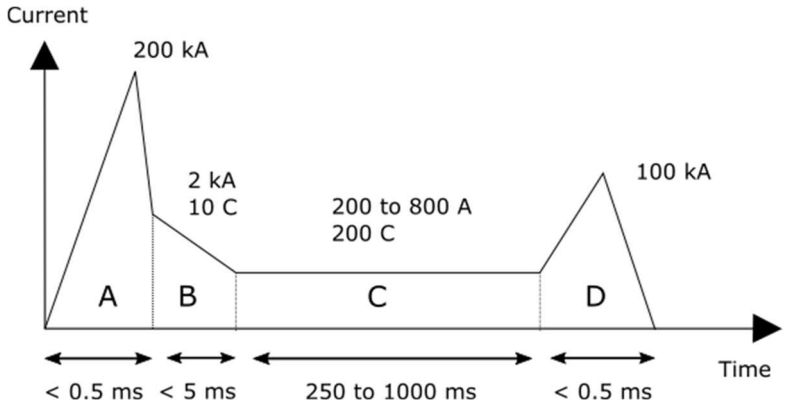

Fig.1. The standardized lightning current waveforms

However, as during the continuous phase the arc has a relative motion to the aircraft due to the airflow, the arc root does not dwell on the same point of the aircraft for the total duration of the C-waveform. Thus, the standards also introduce a truncated C waveform called C* that is simply a shorter version of the C-waveform: its intensity is 400 A in average, maintained for 5 to 50 ms thus delivering 2 to 20 C.[10] The standard also states a charge transfer of ±20% around the setpoint. To ensure the respect of these boundaries, the objective in this work is to limit variations of ±10% around the 400 A setpoint current level. This more severe limitation will enable accurate physical parameter estimations in further experimental studies.

This relative motion between the arc and the aircraft also triggers considerations about the length of the arc column for the representability of the phenomenon. Indeed, during the lightning strike, the steady arc column is elongated in the crossflow direction until it reattaches to another point of the aircraft fuselage. The reattachment of the lightning channel is referred as restrike when the arc roots leaps from one attachment point to another or as swept stroke when the arc roots glides on the surface. At atmospheric pressure and with air injection, Wutzke *et al.*[11] measured a minimum relative velocity of 20 m/s above which the electric arc channel diverts from a steady column and is subject to reattachment. These experiments were led using copper as electrode material and performing electric arcs of 100 A and 10 mm. So, in order to reproduce experimentally a lightning restrike with a relative velocity of 20 m/s and respecting the 50 ms arc duration recommended by the standards, the minimum length of the electric arc has to be 1 m. Therefore, the objective of our lightning generator is to reproduce an electric arc of 1 m respecting the standard C*-waveform – a 400 A average intensity with a maximum variation of ±10% during 50 ms. Moreover, when the arc length is extended due to a relative motion between the arc and the aircraft, its electrical potential increases.[12] When restrike occurs, as the length of arc suddenly decreases, its electric potential does as well and the lightning generator has to be robust enough to provide a regulated current of 400 A respecting the standard C*-waveform. Indeed, using a rocket sled Dobbing and Hanson[13] propelled a test vehicle at a speed of 72 m/s through a 600 A

stationary arc and observed a voltage drop of 3.2 kV in less than 4 ms (4 ms being their smaller timescale step) occurring during a restrike.

B. Other lightning generators published for C-waveforms

Few references of other lightning generators are available in the literature. Whereas the high-current transient A, B and D waveforms issued from the lightning standard can be reproduced using passive electric circuits – Sousa Martins *et al.*[14] and Leichauer[15] present a RLC circuit triggered by a spark-gap and Kovalchuk *et al.*[16] present an adapted Marx generator – C-waveform can be released with active and passive circuits. Caldwell *et al.*[17] use a motor/generator set that is spun up and that generates hundreds of amperes when released. Dobbing et al.[13] store 700 A in a 3 tonnes and 0.56 H coil with lead acid batteries and discharges it to produce arcs up to 5 m long with a current decreasing from 700 to 350 A in 50 ms. Leichauer[15] presents a Buck converter using a PWM mode with a frequency of operation of 5 kHz that produces a square shaped current waveform of 200 A with a margin of ±25% and lasting 1 s through a 2 Ω resistor.

C. Electrical model of a C-waveform lightning component*

Neglecting the phenomenon of plasma sheath that is located at few hundreds of micrometers in the vicinity of the electrodes, the common electric model of the electric arc consists in time-varying resistor. This model is all the more relevant the longer the arc column is.[18-20] In particular, Sunabe *et al.*[21] measured the equivalent arc resistance for a range of current values of few hundreds of amperes. A domain of interelectrode distance from 0.6 to 3 m for current from 50 A to 10 kA is investigated and the mean electric field and linear resistance (assuming the arc channel is axisymmetric) are given for integration times over 100 ms. These experiments show a linear arc resistance of 5 Ω/m for a current of 200 A and 2.4 Ω/m for a current of 400 A. In his simulations of the electrical mean resistance value of a DC arc Chemartin[22] indicates a mean value of 4 Ω/m for 500 A electric arcs considering the first 50 ms of arc lifetime. So, in order to take into account the upper estimation of resistance for an electric arc at 400 A, a 4 Ω equivalent resistor is considered to model a 1 m long arc at 1 atm and for the duration of 50 ms.

Meanwhile, the high-current that goes through the arc provokes self-induced Lorentz forces that form loops in the shape of the arc column so that it cannot be considered a straight axisymmetric column.[23] The real length of the arc column is thus more important than the distance between the arc electrodes. Tanaka *et al.*[24] show experimentally that a factor 1.6 must be added for DC arc currents of 100 A over the inter-electrode length to represents the real length of the arc. Tholin *et al.*[12] numerically estimate this factor to be 1.8 for 400 A DC electric arcs. Thus, in order to design a lightning generator that would be robust enough to provide energy to a 400 A DC arc of 1 m during at least 50 ms, an electric behavior model of an 8 Ω resistor is chosen considering a factor 2 over the inter-electrode length to take into account the tortuosity shape.

TABLE I. Electrical characteristics of the C*waveform studied in this work.

Current (A)	Equivalent resistor (Ω)	Time duration (ms)	Charge (C)	Current margin (%)	Maximum/Minimum Current (A)
400	4-8	50	20	10	440/360

D. Discussion on the source of energy

An 8 Ω resistor that is traversed by a 400 A current requires a source of energy that could provide an electrical power of approximately 1.3 MW. Such a level of electrical power cannot be delivered by a simple laboratory three-phase grid power. Thus the energy has to be stored in an intermediate energy source that could provide such a power.

Banks of batteries have long been used as a DC source and the technology is well established. Their main advantages are their high energy densities, their ease of use and their prices. But as the experiment is being conducted indoor, this technology gets many drawbacks: this necessitates a high maintenance level with a cooling system and a ventilation system for the escaping hydrogen gas and implies many security issues. A Flywheel could be an interesting solution for high power systems but the cost of the corresponding infrastructures does not make it the best option. Loading energy in an inductive coil is also an interesting option for its high density of energy: a capacitor or a battery is used to accumulate magnetic energy in the form of current through the coil and this energy is suddenly released to the system. In our case, as a maximum current variation of 10% of the setpoint current is permitted for 50 ms, the characteristic electric time $\tau = L/R$, with L being the inductance value and R the load resistance, of the energy discharge has to be around 10 times the arc duration time 50 ms. As the equivalent resistor of the circuit is 8 Ω, this would result in an inductance value of around 4 H to have a τ of 500 ms. A simple model of infinite solenoid shows that for an air coil of copper component, considering the coil wire has a sufficient section size so that its resulting resistance is less than 1 Ω, this equipment could weigh up to several tens of tones and occupy several m^3 of space. This would be too difficult to manipulate in a laboratory.

The most interesting solution for our problem resorts to capacitive energy storage as for their safety advantages - they can be drained out of energy and can be utilized indoors – that for their use of ease. Also, they do not require much maintenance, are compact and are relatively fast to load. Their main drawback for the detailed application is that they do not provide a DC current when connected to a resistor. This can be solved using DC/DC converter topologies that will be discussed in the next section. Their only counterpart is that their main fast-switching components, the high-power IGBT and diode, have a limited operative voltage. For the available high-power components in the laboratory, the model of IGBT chosen has a limit operative voltage of 4.5 kV. Considering an energy transfer from the capacitor energy storage to the electric arc resistor without any losses, the minimum capacitance value that is required to limit the voltage level is given by:

$$C = \frac{2\,RI^2\Delta t}{V^2} \tag{1}$$

where R, I, Δt and V are respectively the equivalent arc resistor (8 Ω), the average current (400 A), the required duration time (50 ms) and the maximum voltage of the capacitors (2.5 kV). This results in a minimal capacitance of 60 mF. In this work, a bank of 5 capacitors of 22.5 mF each and with maximum voltage of 2.5 kV for a resulting capacitance of 112.5 mF is used to grant some leeway and is presented in the following sections.

The main objectives of this paper are to design through simulations and to build a lightning generator that would be able to generate a 400 A DC electric arc of 1 m long during 50 ms. Section I has introduced the electrical behavior in terms of electrical components of an electric arc with the mentioned characteristics. Section II aims to compare the performances of the different DC/DC high-power converters circuits through simulations with a minimum energy criterion. Section III discusses about the experimental implementation of the selected circuits and deals with the transient overvoltage problems with the design of a snubber circuit. In Section IV, the different measurements and results of

the generation of a C*-waveform using an equivalent resistor and a real electric arc are presented with a comparison and discussion of the experimental performances of the different circuits.

II/ Theoretical comparison and design of high-power Generators

A. Context and Adaptation

DC/DC converters are electronic circuits that convert a source of direct current from one voltage operative level to another. There are different kinds of topologies, but they all use the same conversion pattern with few variations: a switch enables to shift the circuit from an Off-state to an On-state so that the source of energy – a capacitor bank in our case – provides energy with a regulation on the current level to the load – an arc equivalent resistor. Standard schemes involve a coil that helps to slow down the current variations and to provide an intermediate storage of energy and also a diode that regulates the current flow.

The converter topologies compared in this paper are presented in Fig. 2. In the Buck configuration, when the switch is activated in Fig. 2(a), the energy from the capacitor is discharged in the load resistor through the coil. When the switch is deactivated in Fig 2(c), the current is maintained in the load resistor passing through the coil and a free-wheeling diode. In the Buck-boost configuration, when the switch is activated in Fig 2(b), the capacitor discharges its energy in the intermediary coil whereas the current is maintained in the load resistance thanks to a filter capacitor. When the switch is deactivated in Fig. 2(d), the energy stored in the coil is discharged through the resistor and the filter capacitor.

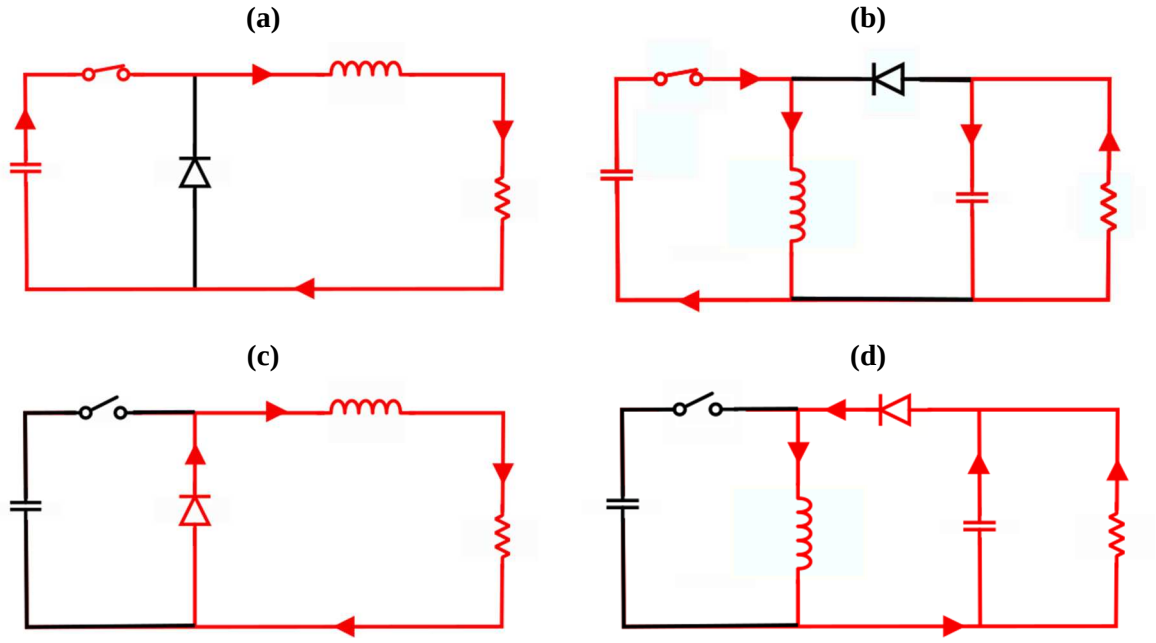

FIG. 2. Presentation of Buck on-state (a), Buck off-state (c), Buck-boost on-state (b) and Buck-boost off-state (d)

Buck converter is referred to as a step-down converter because it steps down the voltage of the supply to the load. Thus, the operative voltage of the load resistors – the electric arc in this application - is limited by the maximum voltage of the supply capacitors. Buck-Boost converter is able to function as a step-down or a step-up converter so that the operative voltage of the load resistor is able to outreach the maximum voltage of the supply capacitors.

The main utilization of DC/DC converters consists in controlling the output voltage by implementing a fixed duty cycle using a PWM mode.[25] As in this application the objective is the reproduction of the C*

current waveform, the focus is the regulation of the load current. Then a closed loop command structure has been selected: the current in the load is measured and depending on its value, the switches enable the circuit to provide energy to it or not, increasing or decreasing its current level, thus creating the regulation.

B. Theoretical comparison of the Buck and Buck-boost performances

In order to compare the different topologies, our criteria are, from the available capacitor bank of around 110 mF, the minimum voltage – and thus the minimum energy – that is required for maintaining a current of 400 A through resistors of 4 Ω and 8 Ω – that are, respectively, upper bound values of electric arcs of 50 cm and 1 m, as mentioned in previous section, during at least 50 ms. The current variation must not exceed 10% of the setpoint current. As all the topologies resort to a load inductance that help to smooth the current waveform, the analysis also has to consider the minimum value of inductance *L* that is required for every configuration.

In the simulation, the topology of RLC-circuit, Buck circuit and Buck-Boost circuit are compared – the RLC circuit not being a proper DC/DC converter but serving here as a reference case. For all the topologies, the algorithm that is implemented for simulations consists in calculating the electric parameters of currents and voltages in every node and branch at the different instants of commutation of the switches, and the different durations of On-state phases (the time duration the circuit requires to increase its load current from 360 A to 440 A) and Off-state phases (the time duration the circuit requires to decrease its load current from 440 A to 360 A). The varying parameters are the initial voltage in the source capacitor bank and the inductance value.

The algorithm equations are represented with the associated schematic diagrams in Fig. 3. During On-phase, the average load current I_R is 400 A and the load current variation ΔI_R is 80 A for the Buck and -80 A for the Buck-Boost whereas during the Off-phase, the load current variation is -80 A for the Buck and 80 A for the Buck-Boost. For every iteration, the algorithm calculates the new values of the node voltage of the bank capacitor U_C and of the coil branch current I_L and the phase duration Δt. The iteration number is referred as n in the equations presented.

(a)

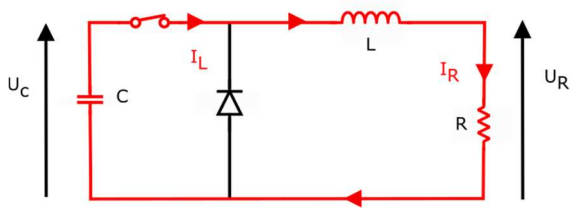

$$U_R = R\, I_R$$

$$\Delta U_R = R \Delta I_R$$

$$I_L = I_R$$

$$\frac{U_C^{n+1} + U_c^n}{2} - U_R = L \frac{I_L^{n+1} - I_L^n}{\Delta t^n}$$

$$I_R = C \frac{U_c^{n+1} - U_c^n}{\Delta t^n}$$

(b)

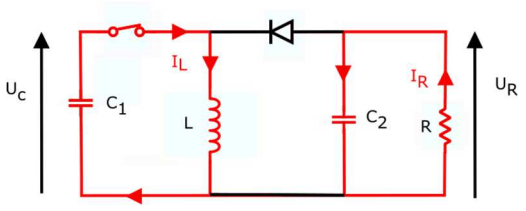

$$U_R = R\, I_R$$

$$\Delta U_R = R \Delta I_R$$

$$I_R = C_2 \frac{\Delta U_R}{\Delta t^n}$$

$$\frac{U_C^{n+1} + U_c^n}{2} = L \frac{I_L^{n+1} - I_L^n}{\Delta t^n}$$

$$\frac{I_L^{n+1} + I_L^n}{2} = C_1 \frac{U_c^{n+1} - U_c^n}{\Delta t^n}$$

(c)

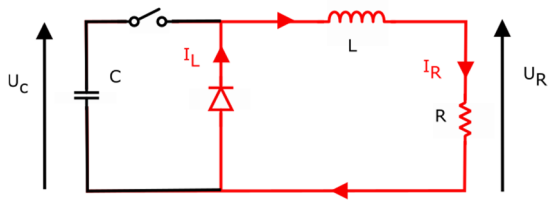

$$U_R = R\, I_R$$

$$\Delta U_R = R \Delta I_R$$

$$I_L = I_R$$

$$-U_R = L \frac{I_L^{n+1} - I_L^n}{\Delta t^n}$$

$$U_C^{n+1} = U_C^n$$

(d)

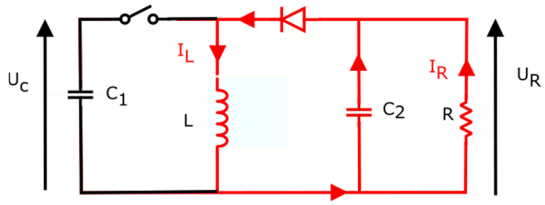

$$U_R = R\, I_R$$

$$\Delta U_R = R \Delta I_R$$

$$U_R = L \frac{I_L^{n+1} - I_L^n}{\Delta t^n}$$

$$\frac{I_L^{n+1} + I_L^n}{2} - I_R = C_2 \frac{\Delta U_R}{\Delta t^n}$$

$$U_C^{n+1} = U_C^n$$

FIG. 3. Electrical equations of the Buck on-phase (a), Buck-Boost on-phase (b), Buck off-phase (c), Buck-Boost off-phase(d).

Table II summarizes the minimum initial bank capacitor voltage and the minimal inductance coil values for which the different topologies under test can generate a regulated current of 400 A with a ±10% margin through respective load resistor values of 4 and 8 Ω for at least 50 ms.

TABLE II. Results of the electric performances of the different topologies

Topology	Equivalent resistor (Ω)	Time duration (ms)	Capacitor Voltage (V)	Coil Inductance (mH)
RLC	4 (8)	50	1900 (3500)	70/90
Buck	4 (8)	50	1900 (3500)	1
Buck-Boost	4 (8)	50	1000 (1500)	1

It can be concluded from this table that the circuit that reaches the best performances for our problem in terms of energy efficiency is the Buck-boost topology. It can match the criterion charging the capacitor bank to only 1 kV for a 4 Ω load and 1.5 kV for an 8 Ω load thanks to the use of the intermediate coil that is able to transform the capacitive energy into inductive energy with better energy density. The use of inductive energy decouples the voltage level of the capacitors from the voltage level of the equivalent arc load resistance. Indeed, in the Buck configuration, the initial voltage in the capacitors needs to be superior to the arc voltage of 3.2 kV resulting from a 400 A current flowing through an 8 Ω resistor.

In the other hand, the inductance value given by the RLC configuration value is in the order of magnitude of 0.1 H, which would result in a coil mass of more than one tonne to keep a resistance inferior to 1 Ω. So, despite RLC circuit has the advantage over DC/DC converters of not requiring any power switch IGBT or power diode, it is excluded in the rest of this work.

Looking closer to the Buck-boost configuration, the conversion of the capacitive energy to inductive energy is only effective if a high level of current is stocked in the intermediary coil – reaching up to a few kA in our configuration. This represents a non-negligible problem because the available power switches IGBTs have a 1.2 kA current limit. A solution for this issue is to add several of these components in parallel. Two IGBTs were added in parallel for the Buck-Boost configuration to reach an operative current of 1.5 kA but this solution increases driver issues and costs. The solution implemented in this paper is to add another feedback-loop regulation on the current that flows into the coil that has a priority over the one regulating the load current, so that the switch components are protected from a level of current they cannot endure. Meanwhile, if the priority is given to the intermediary coil current, the load current square form is inevitably deteriorated as the only way to prevent a surge of current in the coil is to discharge it in the load resistance. However, this might be acceptable and stay in the limit of the 10% margin over the set point current value. This issue will be treated in the following sections.

Another problem with the Buck-Boost configuration is that the voltage at the terminals of the IGBTs devices is higher than the initial voltage of the bank capacitor because of the inversion of polarity of the load resistance whose high voltage point is referred to the circuit mass. Consequently, when IGBTs devices switch off, one of their terminals is raised to the voltage level of the capacitor bank V_{CAP} whereas the other terminal is referred to the negative voltage point of load resistance V_{ARC} = - R I_{ARC} with R being the equivalent arc load resistor. Thus, the voltage between the terminals of the IGBT´s devices is given by:

$$V_{IGBT} = V_{CAP} + R\, I_{ARC} \quad (2)$$

Considering the values of Table II for respective equivalent load resistors of 4 Ω and 8 Ω, this voltage reaches 2600 V and 4700 V. The value of 4700 V is inacceptable as operative voltage because it is over the IGBTs voltage limit. The resume of operative voltages and currents of Buck and Buck-Boost configurations main components to reproduce a C*-waveform of 400 A is given in Table III.

TABLE III. Comparison of Buck and Buck-Boost components operative voltages and current

Topology	Equivalent resistor (Ω)	Capacitor initial voltage (V)	IGBTs operative voltage (V)	IGBTs operative current (A)	Feedback loop regulations
Buck	4(8)	1900(3500)	1900(3500)	400	1
Buck-Boost	4(8)	1000(1500)	2600(4700)	1500	2

III/ Experimental set-up and design of a snubber

A. Description of materiel under-test

The same equipment has been used for the both Buck and Buck Boost topologies: This consists of a capacitor bank composed of five capacitors of maximum voltage 2.5 kV and with 22.5 mF each, another capacitor bank composed of two capacitors of 10 mF each and with a maximum voltage 5 kV, an air-coil of a variable inductance from 2 to 10 mH for an internal resistance of only 30 mΩ with a total weigh of 300kg, single switch IGBT modules from Dynex Semiconductor (DIM1200ASM45-TS000) that possess a collector-emitter maximum voltage value of 4.5 kV and a maximum continuous collector current of 1.2 kA, fast recovery diode modules from Dynex Semiconductor (DFM750AXM65-TS000) with a maximum repetitive peak voltage of 6.5 kV and a total forward current of 2.25 kA (750 A per arm).

The current measurements are realized using a PEM CWT AC CWT60LF probe. The voltage measurements are made using voltage probes of reference North Star PVM-1 - and of reference Lecroy PPE5KV.

Figure 4 presents photography of the high-power lightning generator assembled; the red cylindrical coil has been moved 3 m away using long wire so that its magnetic field does not disturb the signals of the electronic microcontroller closed-loop part of the generator.

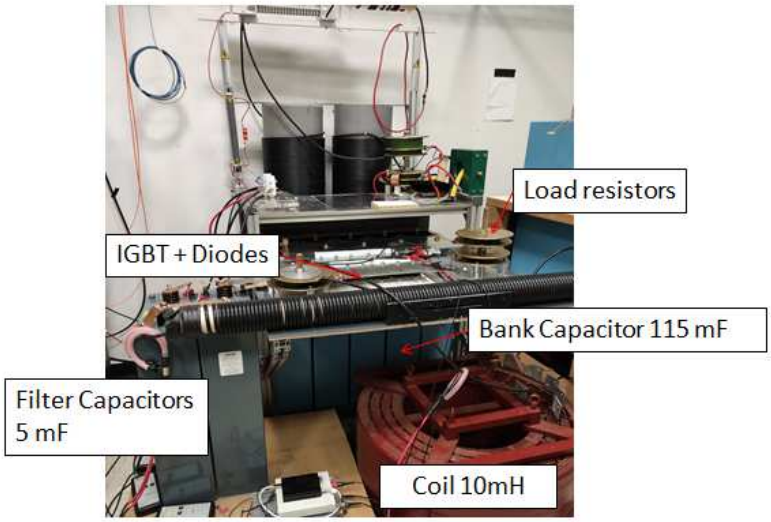

FIG. 4. Assembly of the high-power lightning generator

Feedback-loop regulations are implemented for the load current in the Buck topology and for both the load current and the intermediary coil current in the Buck boost topology. It involves one or two measurements of current, a treatment and a comparison to a setpoint value from a microcontroller and a communication to the IGBT switch to activate or deactivate it as depicted in Fig. 5.

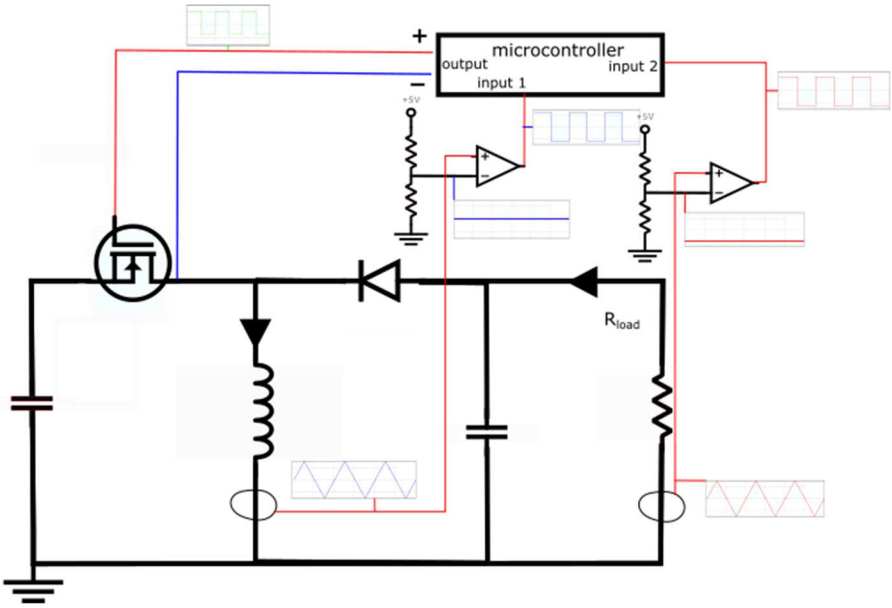

FIG. 5. Schema of feedback loop of Buck-boost circuit

B. Transient Overvoltage problems and snubber design

First, lightning generator regulation loop principle is tested and characterized experimentally at low power (a few hundreds of volts maximum in the energy source capacitor bank for setpoint currents of a few hundreds of amperes) for both Buck and Buck-boost configurations. Peaks of voltage of hundreds of volts that are not predicted by the simulation models are appearing at the IGBT terminals, especially during the switch-off phases. Indeed, a configuration of a capacitor bank of 10 mF initially charged at 400 V and using an air-coil of 2 mH (internal resistance of 0.5 Ω) and aiming to discharge a regulated

200 A current in a 0.1 Ω load was carried out. Figure 6 represents the experimental graphs obtained for this configuration with the Buck circuit.

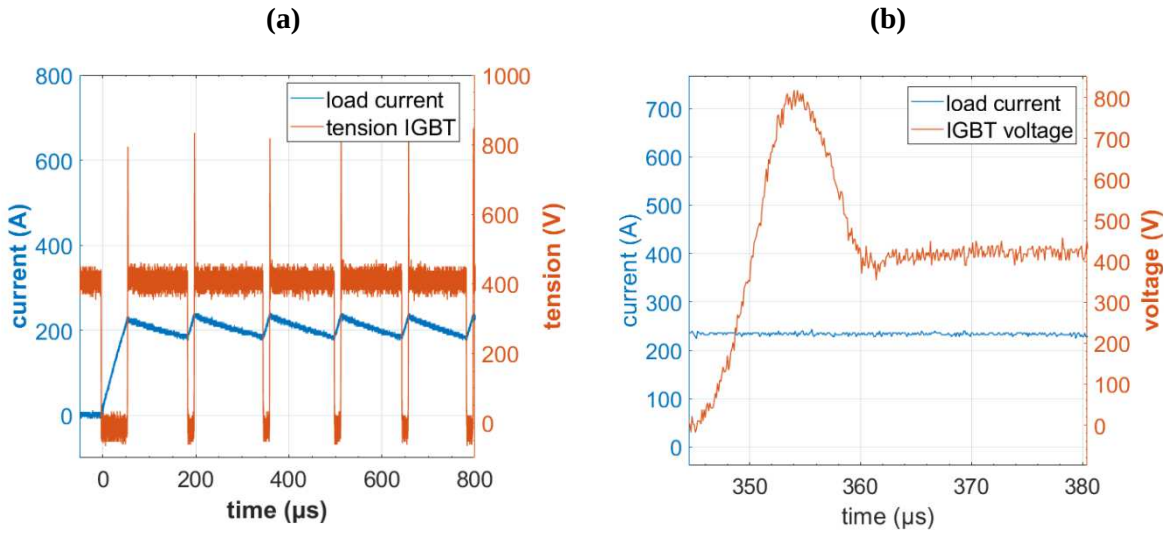

FIG. 6. Presentation of experimental curves with Buck configuration for low power applications (a) shows the overvoltage peaks of IGBT for 5 commutations and (b) is a zoom of one overvoltage peak.

As it can be seen in the curves, the overvoltage can reach almost 2 times the initial voltage level in the capacitors – reaching a value higher than 700 V in the Buck topology for an initial voltage of 400 V. So, expecting to charge the capacitors to an initial voltage of 2 kV as required for an electric arc of 1 meter minimum, an overvoltage peak of 4 kV might be expected in case of a proportional overvoltage peak.

This overvoltage peak issue is a wide subject of studies in the area of power converter circuits and is mainly caused by peripheral parasitic inductances.[26,27] Indeed, in both Buck and Buck-boost configurations, when the IGBT converter switches off, the current that goes through the loop involving the source energy bank capacitor and the IGBT suddenly drops from a value up to 400 A for Buck configuration (1500 A for the Buck-boost case) to zero. And when the IGBT converter switches on, the current that goes through the loop involving the diode suddenly drops as well.

Considering the inductance formed by this branch composed by the parasite inductances of the IGBT device and of the capacitor bank, and by the wire's equivalent inductance, this steep variation of current provokes the apparition of an overvoltage peak expressed by the following equation [26]:

$$V = L_p \frac{\Delta I}{\Delta t} \tag{3}$$

with V being the transient overvoltage, L_p being the total peripheral parasitic inductance and ΔI being the current variation during the switch-off phase and Δt being the turn-off delay time (3.1 µs for the described model of IGBT module).

Power switch technologies are usually protected from this overvoltage peak resorting to damping circuits called Snubber circuits. Amongst other advantages, it also reduces the electromagnetic interferences (EMI) that could affect the circuit and the commutation losses of the switches.[28] The two main kinds of snubber filters are the Resistor-Capacitor (RC) and Resistor-Capacitor-Diode (RCD) damping circuits and consist in converting the magnetic energy of the parasite inductance circuit in electric energy through a capacitor placed in parallel to the switch.[29] The resistor and the diode enable to control the flow of current going from the switching circuit to the snubber circuit.

The snubber capacitor must have a capacitance (C_{snub}) as low as possible to be able to evacuate quickly the overvoltage peak in a RC circuit but also high enough to damp the magnetic energy from the parasite inductance. Thus, the C_{snub} parameter of the RC circuit is given by equation[29]:

$$C_{snub} = \frac{L_p \Delta I^2}{\Delta V^2} \tag{4}$$

with ΔI being the absolute current variation during the switch-off and ΔV the maximum overvoltage peak acceptable at the terminals of the IGBT switch. Thus, a capacitance snubber value can be designed only with access to the total peripheral parasitic inductance.

The total peripheral parasitic inductance can be roughly evaluated by a geometrical model of the circuit to determine the wire inductance as done by Yamashita *et al*[26]. It can also be evaluated experimentally measuring a ringing cycle between the inductance circuit and a known value capacitor placed at the terminal of the IGBT switch during a switching-off phase[29]. This last method is implemented in this work: different values of capacitance *C* have been added in parallel to the switch. Measuring the frequency of the ringing cycle from the capacitor to the parasitic inductance, a mean value of L_p is determined with:

$$\mathrm{L_p} = \frac{1}{4\,\pi\,\mathrm{f}^2 \mathrm{C_{test}}} \tag{5}$$

where *f* is the ringing frequency experimentally measured and C_{test} is the value of the test capacitance. Figure 7 presents the curves obtained with Buck configuration for different values of *C* as a test capacitor and shows the ringing phenomenon. The dataset and the measured values of the ringing frequency and the estimation of L_p are summarized in Table IV. The additional stray inductance brought by the paralleling of the different test capacitors is neglected is this calculation because the capacitors terminals have been welded directly on the IGBT switch terminals.

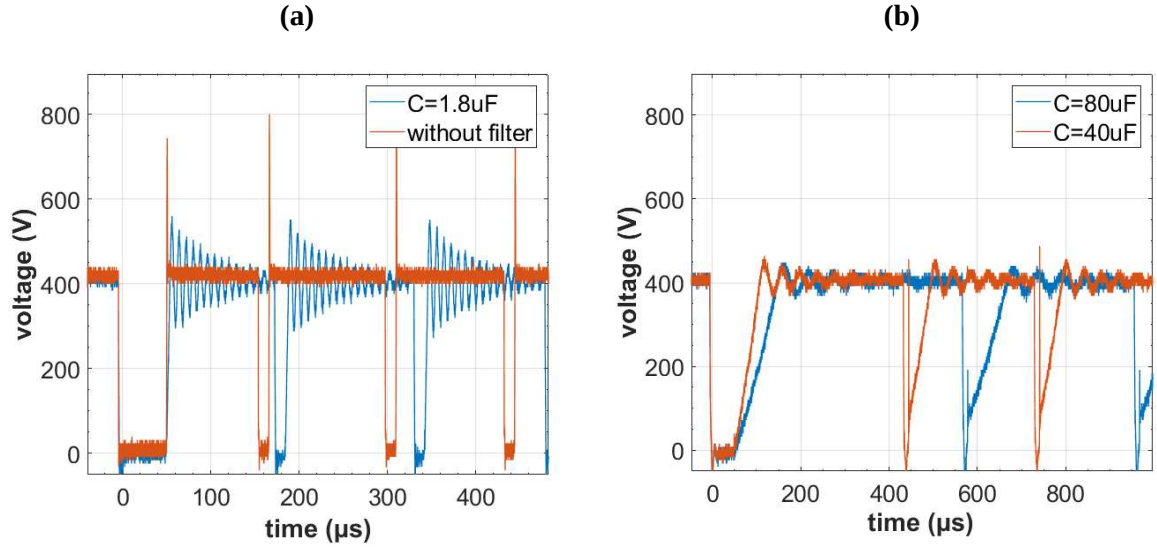

FIG. 7. Presentation of the ringing phenomenon using different values of C*:* (a) without filter and with C = 1.8 µF and (b) with C = 40 µF and C = 80 µF.

TABLE IV. Experimental determination of L

Capacitor value (µF)	Frequency of ringing (kHz)	Parasitic Inductance (µH)
1.8	125	0.9
40	25	1.01
80	18	1.03

The experimental results give a parasitic inductance in the order of magnitude of 1 µH. It appears also from those results that the addition of a capacitor in parallel to the switch is already sufficient to damp the switching-off overvoltage. However, this simple option is dangerous and stresses the IGBT switch as during the switch-on phase the energy accumulated by the parallel capacitor is discharged back in the IGBT without any current limitation. This discharge is a potential source of breakdown for the device. For this reason, most snubber circuits possess a resistor that limits this current. Considering that the variation of current is up to 400 A in the Buck circuit and 1500 A in the Buck boost circuit when the IGBT switches-off, the maximum overvoltage peak acceptable being set at 100 V and with the parasitic inductance mean value of 1 µH, snubber capacitors of respective capacitance values 16 µF and 190 µF can be chosen using Eq. (4).

From these values of capacitances, a RCD-snubber circuit is added in parallel to the switches. Its operation is represented in Fig. 8. During the switch-off phase, the current going through the parasitic inductive circuit do not abruptly vanishes but is able to charge the snubber parallel capacitor passing through the diode module as shown in Fig. 8(a). The diode is advantageous here: it enables to by-pass the resistor so that the peak of voltage is rapidly absorbed by the capacitor and no energy is lost in the resistor. During the switch-on phase, the snubber capacitor gives back its energy, discharging its current through the IGBT as shown in Fig. 8(b) – the resistor value being chosen so that the current intensity remains in acceptable levels.

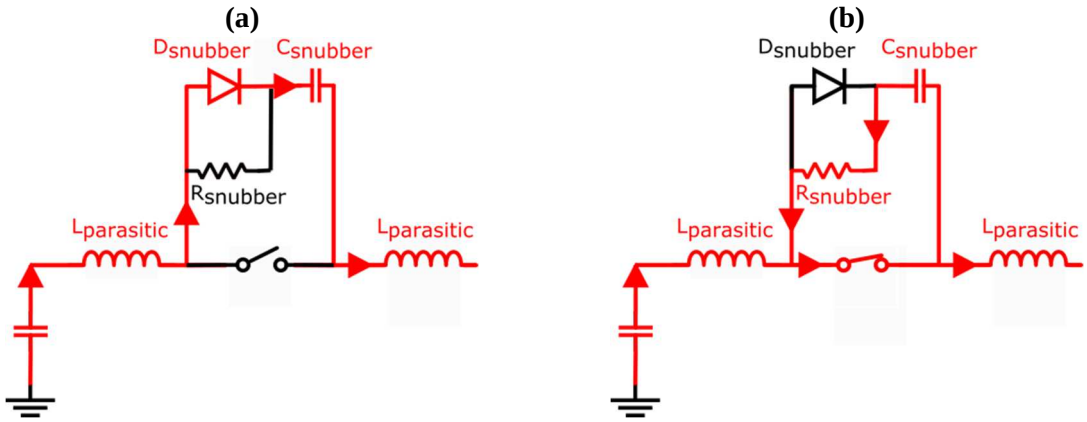

FIG 8. Representation of an RCD-circuit operative damping of overvoltage peaks during (a) switch-off phase and (b) switch-on phase.

To ensure an efficient damping, the cycle composed by the charging and the discharging phases of the snubber capacitor must be faster than the cycle of switch-on and switch-off phases of the IGBT. Indeed, if the capacitor does not evacuate all its energy during the switch-on phase, it would be partly charged during the next switch-off phase and might not be able to damp the magnetic energy – and so the overvoltage peak - of the next cycle. This problem is illustrated in Fig. 9 with the Buck-boost configuration. In Fig. 9(a), a snubber RCD of values C = 100 µF and R = 1 Ω is implemented whereas in Fig. 9(b), a snubber RCD of values C = 100 µF and R = 10 Ω is implemented. During the switch-off

phase, the current that is stocked in the snubber capacitor is measured positively and the overvoltage in the terminals of the IGBT is reduced. During the switch-on phase, the capacitor discharges its energy with a RC time constant of 100 µs in Fig. 9(a), reaching a peak current value of 300 A and a RC constant of 1 ms for a peak current of 30 A in Fig. 9(b), those current peak levels are linked with the operating voltage V (300 V in this example) and the snubber resistance R by $I_{peak} = V/R$. It can be observed that in the Fig. 9(a), the current going out of the snubber capacitor drops to zero before the next switch-off phase and no overvoltage peak occurs in this next phase whereas in Fig. 9(b), the current does not drop to zero at the switch-off phase and an overvoltage transient peak is observed. However, the peak of current that occurs during the discharge of the snubber capacitors is traversing the IGBT in addition to the operating current and stresses the device. Thus, an overvoltage peak level has to be accepted to limit this peak current as a compromise.

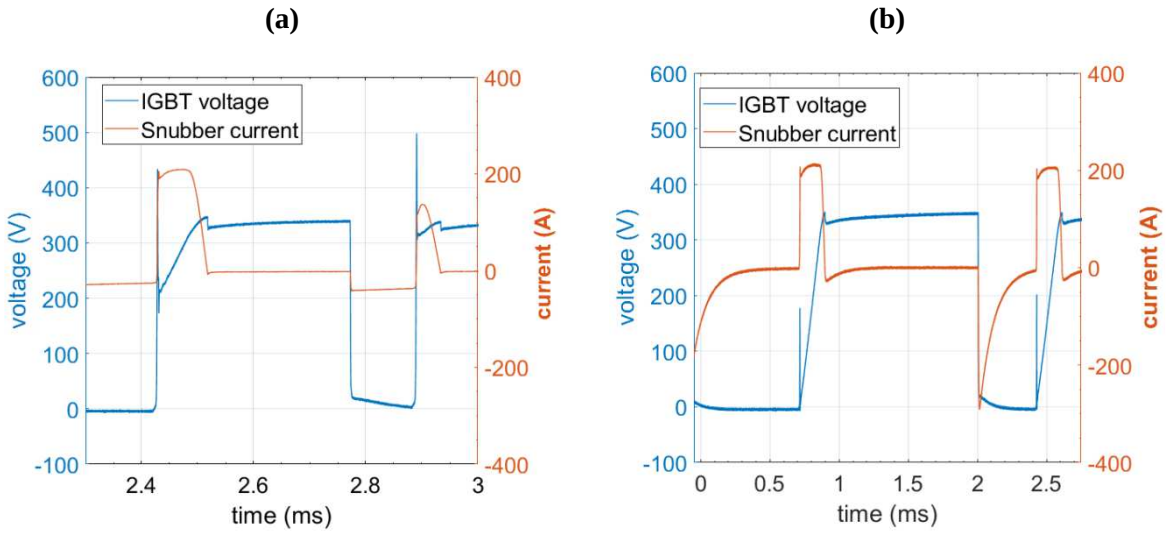

FIG 9. Comparison of two snubber designs with C = 100 µF and R = 10 Ω (a) or R = 1 Ω (b).

Another solution is to reduce artificially the frequency of the regulation adding a delay in the microcontroller code so that the switch-on phase lasts longer than the RC snubber discharge. This idea is illustrated Fig. 10. For the Buck-boost configuration, a frequency limitation is established to switch the IGBT – 50 kHz in Fig. 10(a) and 250 Hz in Fig. 10(b). In Fig. 10(b), a RCD snubber is implemented, with R and C values of 10 Ω and 100 µF respectively. In both configurations, the setpoint load current is 200 A and the limitation current in the intermediary coil is set to 800 A. In Fig. 10(a), it can be observed that the setpoint current is respected, with a maximum variation of 10 A (5%), but the overvoltage peaks reach over 1 kV in Fig. 10(c) whereas in Fig. 10(b), the maximum variation is 100 A (50%) of the setup current but the overvoltage peak does not exceed 100 V in Fig. 10(d). Thus, a compromise must be found between the acceptable overvoltage peak level and the regulation of the current waveform.

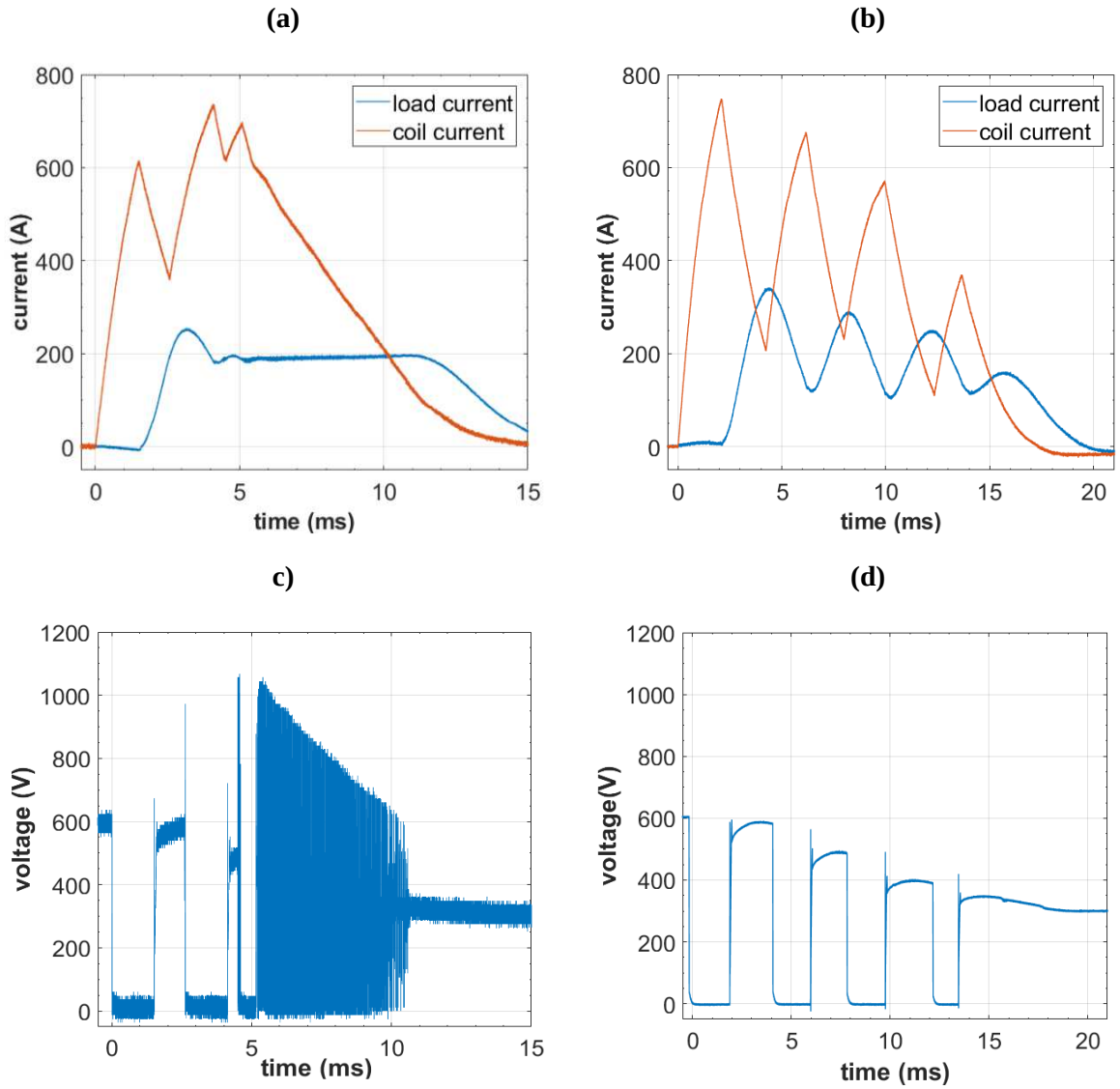

FIG. 10. Comparison of current waveforms and overvoltage peaks for switching frequencies of 50 kHz (a), (c) and 250 Hz (b), (d).

In addition, to minimize this overvoltage peak in the high-power level experiments, an effort is made to reduce the peripheral parasitic inductance changing the geometry of the circuit. Indeed, whereas the previous circuits were mainly made of bus bars to connect the components, a second circuit version for high-power tests is built with large and thin plates of aluminum.

IV/ High-Power experiments and Results

A. Experiments with resistor as an arc and comparison of Buck and Buck-boost performances

Before comparing the performances of Buck and Buck-boost topologies in the case of a real lightning arc, a first comparison is made replacing the arc by a 4 Ω resistance. This resistance is supposed to represent, for a current of 400 A, an arc of 1 m according to Sunabe *et al.*[15] and of 0.5 m for Chemartin[15]. For both topology, the initial voltage of the capacitor bank is incremented until finding a setup that could create a C*-waveform (400 A for 50 ms) through the load resistance to respect the energy criterion. A close attention is taken for the tension in the terminals of the IGBT switch and the diode modules to avoid destruction of these components due to commutation overvoltage as discussed in Sec. III. The maximum allowed frequency of commutation is finally set to 5 kHz. Indeed, it turns out experimentally

that it is enough to respect the 10 % margin of current setpoint and because this is one order of magnitude less than the maximum switching frequency of the IGBT, then this component is not stressed. In both configurations, once the current setpoint is reached, the microcontroller stops the regulation algorithm after 100 ms. In the case of the Buck-boost configuration, the efficiency of the regulation also depends on the level of current that is allowed in the intermediate coil. This current is limited to 1500 A as this is the limit level for the coil and for the IGBTs (two IGBT with a limit of 1200 A are placed in parallel in this configuration). Moreover, whereas in the Buck configuration, the current at the load resistance is directly regulated, in the Buck-boost configuration, the intermediary coil is first charged until it reaches its limit current value (1500 A) then, the current in the coil is discharged in the load resistance until the load current reaches the setpoint value (400 A). However, the load resistance might consume all the energy gathered in the coil before it reaches the setpoint value. To avoid this, the IGBT is switched on every 2 ms to reconnect the coil to the capacitor bank and so to reload its current until it reaches again its limit value as long as the load current does not reach the setpoint value. The load current during the switch-on phase is maintained thanks to a 5 mF filter capacitor placed at the terminals of the load. When the load current reaches 400 A, the proper regulation phase starts: the current in the load is regulated except in case the coil current exceeds its imposed limit current. In this last case, the IGBTs switch off and so the coil evacuates its current in the load for 200 µs before the load regulation restarts. Results of Buck-boost and Buck configurations for a 4 Ω resistance are represented in Figs. 11 and 12. In the Buck-boost configuration, the initial voltage is 1600 V and curves of the load and intermediary coil current waveforms are represented in Fig. 11(a), whereas the voltage at the terminals of IGBT and diode are shown in Fig. 11(b) for one commutation. In the Buck configuration, the initial voltage is 2000 V, and the load current waveform is represented in Fig. 12(a), whereas the voltage at the terminals of IGBT and diode are shown in Fig. 12(b) for one commutation.

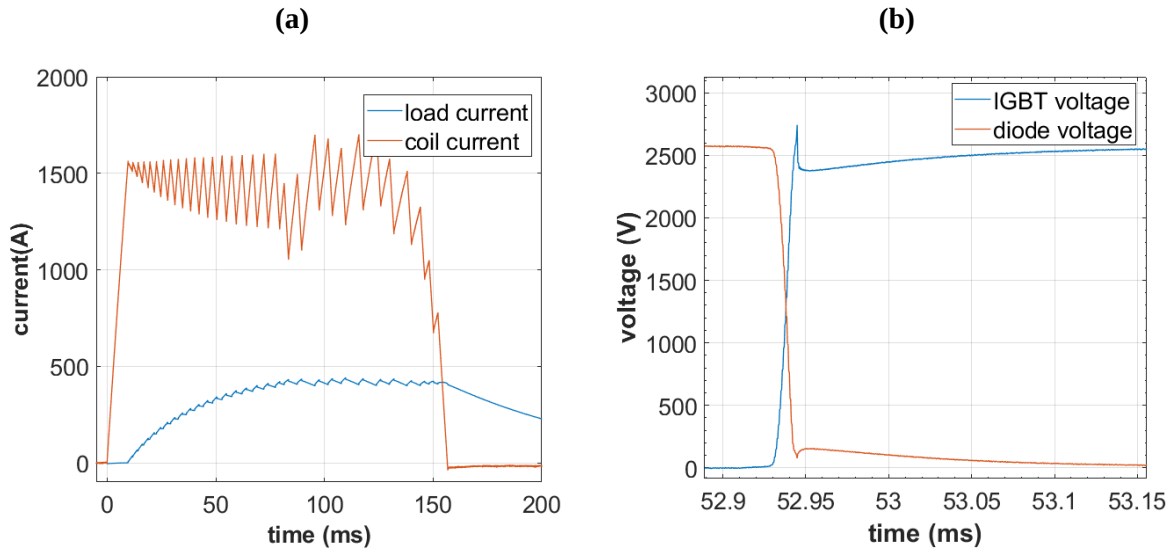

FIG 11. Currents (a) and voltages (b) waveforms of Buck-boost configuration for a 4 Ω load resistance

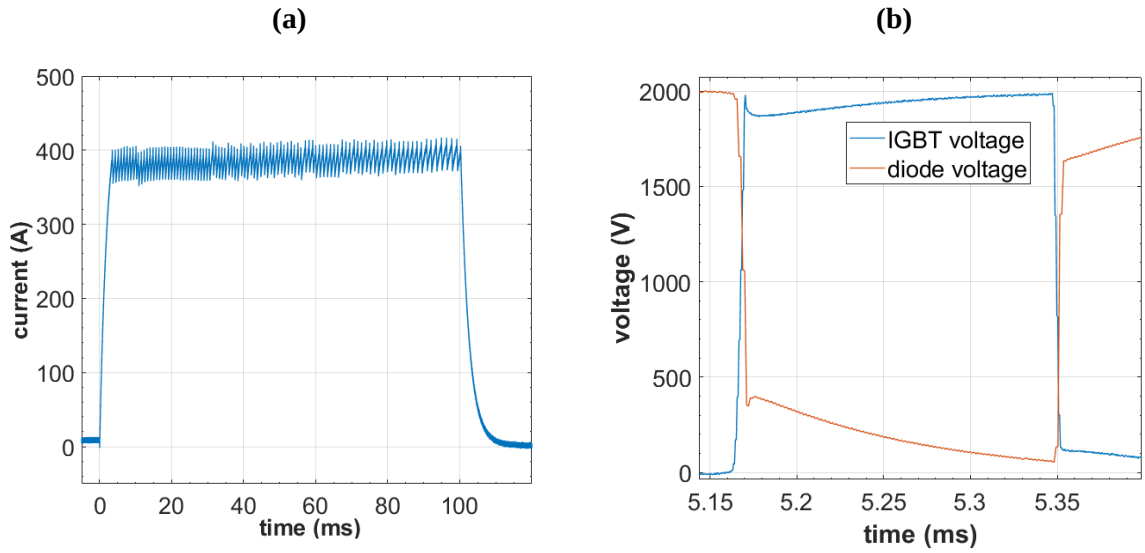

FIG 12. Current (a) and voltages (b) waveforms of Buck configuration for a 4 Ω load resistance

In Fig. 11(a), initially, the IGBT switches on and the capacitor bank charges the coil for 10 ms until this reaches its limit current value of 1500 A. Then, a first regulation phase of the current in the coil starts: the current is sent from the coil to the load resistance during 200 µs and then the coil is reconnected to the capacitor bank until it reaches its maximum value. This regulation lasts until the load current reaches 400 A at 74 ms. Then, the proper regulation of the load current starts and is maintained from 74 ms to 157 ms. In this configuration, the regulation of the load current and the limitation of the coil current are both respected. In Fig. 11(b), voltage waveforms of the same setup are represented at the terminals of the IGBT and diode modules for one commutation. The voltage level at the terminals of both modules – maximum 2800 V – is higher than the initial voltage of the bank capacitor because of the inversion of polarity of the load resistance whose high voltage point is referred to the circuit mass. As discussed in Sec. III the transient overvoltage peaks is measured from Fig. 11(b) and reaches a level of 2800 V whereas the operative voltage of the IGBT reaches 2700 V in the non-transient phase. A 100 V difference voltage is considered acceptable in terms of destruction risks for the switching devices.

In Fig. 12(a), load current waveform of the Buck topology is represented for an initial voltage of 2000 V. The regulation of the load current at a setpoint level is direct and lasts 100 ms until the microcontroller algorithm stops it. In Fig. 12(b), voltage waveforms of the same setup are represented at the terminals of the IGBT and the diode modules for one commutation. Conversely to the Buck-boost configuration, the low voltage point of the dipole resistor is directly connected to the reference mass in this case, and the highest operative voltage point of the circuit is the positive terminal of the capacitors. It can also be observed from Fig. 12(b) that the transient overvoltage peak reaches a level of 2000 V whereas the operative voltage of the IGBT also reaches 2000 V at the end the cycle in the non-transient phase. In this configuration, the effect of the overvoltage peak is shown to be negligible.

Both Buck-boost and Buck topologies enable to perform a regulated C*-waveform of 400 A through a load resistance of 4 Ω. As predicted in the theoretical simulations of Sec. II, an initial voltage level of 2000V is enough to achieve this performance for the Buck configuration whereas the initial voltage level required is highest than expected for the Buck-boost configuration. This is probably due to the current coil limitation that deteriorates the energy conversion from the capacitor voltage to the coil current – the advantage of getting a higher energy density from an inductance source than from a capacitive source is minimized if the level of current is limited. Still, for the same performances, the Buck-boost configuration requires 20% less voltage for the initial load of the bank capacitors, which

represents 36% less energy. In the other hand, the Buck-boost circuit introduces a higher level of operative voltage at the terminals of the switching elements, which remains acceptable for a 4 Ω resistor load.

B. Experiments with electric arcs and comparison of Buck and Buck-boost performances

Figures 13(a) and 13(b) present the performance results of, respectively, Buck-boost and Buck configurations current waveforms with electric arcs instead of a load resistance. The ignition of the electric arc is made using a conductive thin wire that is likely to explode when the current rises in it by Joule effect. This rapidly heats the surrounding air and contributes to generate a lightning-like plasma.[30] The wire is placed between a positive electrode, being a tungsten rod of 10 mm diameter, and a negative electrode consisting of a square aluminum plate of 400 × 400 × 2 mm^3. A high speed camera (HSC) is used to evaluate the arc's shape and behavior. The HSC is a Phantom V711 from Vision Research (CMOS sensor of 1280 × 800 pixels of 20 μm^2) and is set to work with a sampling rate around 20 kfps.

In Fig. 13(a), arc current waveforms of the Buck–Boost topology are represented for an initial voltage of 1100 V, an electric arc of 150 mm as an inter-electrode distance, a setpoint value of 400 A for the arc current and a limit of 800 A for the intermediate coil current. Initially, the IGBT switches on and the capacitor bank charges the coil for 7 ms until it reaches its limit current value. Then, the first regulation phase starts: the current is sent from the coil to the arc resistance. It can be observed that the current in the wire does not increase fast in this phase during the first 31 ms, and then a sudden surge occurs that matches the wire explosion – as it is confirmed by the HSC. This surge reaches the set point current value at 32 ms and provokes the saturation of the current probe that is operative for current levels under 1.2 kA. Then, the regulation of the arc current starts and is maintained until 132 ms. Nevertheless, despite the setpoint value, the arc current is not only unstable – it varies from 250 to 1000 A after the first peak of current – but also has a mean value of around 600 A. This can be explained by the fact that the electric arc does not consume enough energy to evacuate the coil current correctly. Indeed, the coil current regulation has the priority over the arc current regulation to avoid a surge of current in the coil that could damage the switching devices.

In Fig. 13(b), the arc current waveform of the Buck topology is represented for an initial voltage of 2 kV, an electric arc of 1 m as inter-electrode distance and a setpoint value of 400 A of the arc. Figure 14(a) presents the arc voltage waveform for this case and Fig. 14(b) present the time varying resistor of the arc that is obtained by dividing the voltage at the terminals of the arc by the arc current. It can be observed that the current reaches the setpoint value in less than 2 ms whereas the voltage of the arc rises to 2.8 kV. During this time, it has been confirmed by HSC that the ignition wire has not exploded yet. The surge of voltage might be explained by the increase of resistivity of the copper wire at high temperature and when this wire starts phase change due to Joule heating. Indeed, the maximum resistivity of solid copper is reached at temperature 1085 °C just before the fusion point. For a copper wire of 1 m and of 280 µm diameter, it results in a resistance of 1.7 Ω considering the resistivity as a function of temperature. This value, that is inferior to the 8.5 Ω measured in Fig. 14(b), indicates that this surge of voltage can be a result of a phase change effect. At 3.5 ms, the current suddenly drops to 320 A and the voltage to 1.7 kV. The HSC confirms that the wire has already exploded and plasma is forming. Then the current takes 5 ms to reach again the setpoint. From this point, the current is regularized until 100 ms when the microcontroller stops the algorithm, while the voltage variates from 1.7 kV to 1 kV and the arc resistance varies between 2 and 3 Ω. At the end, the current regulation around the value of 400 A lasts more than 90 ms. After the end of the regulation, the arc vanishes and the resistor value measured between the two electrodes increases. No overvoltage peaks are observed at the terminals of the switching devices during the transient switching off phases of the regulation.

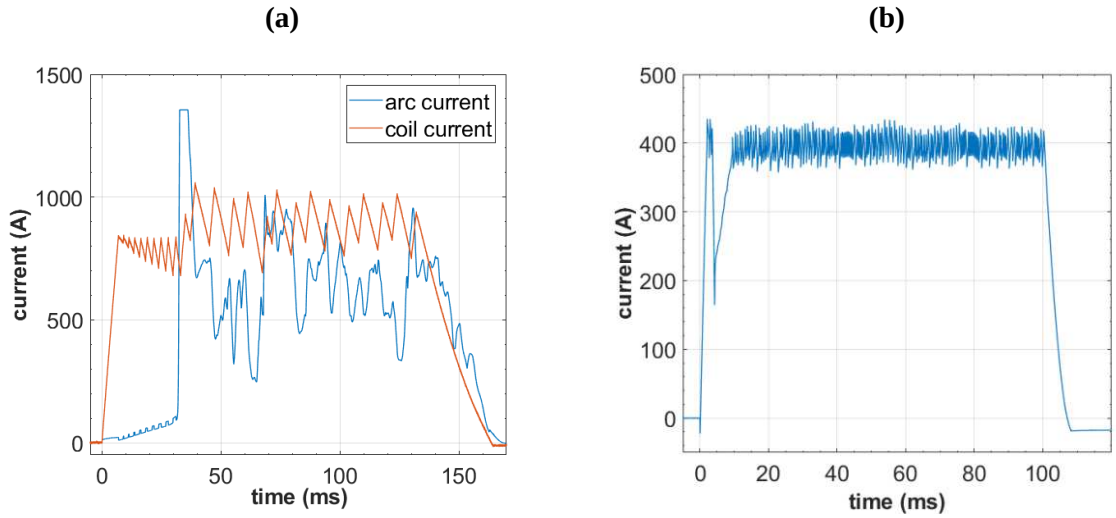

FIG. 13. Current waveforms of Buck-boost configuration for a 150 mm arc (a) and of Buck configuration for a 1000 mm arc (b).

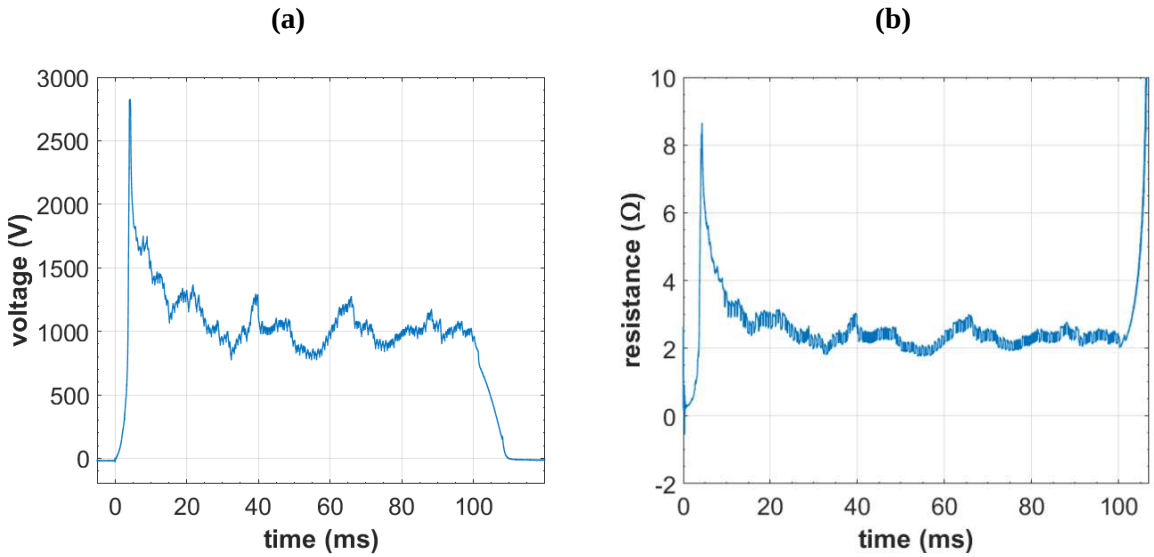

FIG. 14. Voltage waveform (a) and time varying resistance (b) of Buck configuration for a 1000 mm arc.

C. Discussion and Analysis of different topologies performances

These results showed that for a load resistor of 4 Ω, both Buck and Buck-boost configurations can perform the C*-waveform of the lightning standard – with an advantage for the Buck-boost configuration that requires less energy. For the case with electric arcs, only the Buck generator is robust enough to perform this C*-waveform. Indeed, the fact that it has a direct feedback loop on its current level makes it more flexible to the fast variations of the plasma resistance – especially during its ignition phase when the conductive medium changes from a wire of copper at room temperature conditions to high-density plasma. The Buck-boost is less flexible due to his intermediate conversion of energy using a coil. The main problem being that the low-resistance and highly-inductive coil must be limited in terms of energy storage to avoid an operative current higher than a few kA. A simple solution would be to use an external resistive circuit to damp the energy of the coil in case the current in the arc is too high. But adding this extra circuit would have two drawbacks: this would consume energy by damping the coil

current and thus deteriorate the efficiency of the circuit. Also, this would require at least two other IGBT switches in addition to the two ones that are already implemented in the Buck-boost configuration to regulate the flow of current going out of the intermediary coil. As previously mentioned, the IGBT module is the weakest component, using as less units as possible is a preferable strategy. In the end, only the Buck was able to perform a C*-waveform for arcs up to 1.5 m. Table V summarizes the final parameters and components of the Buck generator used for these arcs.

TABLE V. Summary of parameters and components for the selected configuration

topology	Initial voltage (V)	Capacitance (mF)	Stored Energy (kJ)	Coil Inductance (mH)	IGBT peak transient voltage (V)	Current setpoint (A)	Maximum Current ripple (A)	Current duration (ms)
Buck	2300	112.5	298	10	2400	400	±50	100

Based on the work of Sunabe *et al.*[15] and Chemartin *et al.*[16], the linear arc resistance value was firstly supposed to be between 2.4 and 4 Ω/m without considering the tortuosity factor, and between 4 and 8 Ω/m considering it. Therefore, for the Buck configuration, different arc lengths were experimentally reproduced by increasing the inter electrode distance, with a 100 mm increment, and increasing the initial voltage level. The highest length performed with the experimental setup described was 1.5 m with an initial voltage of 2.3 kV, and reminding that 2.5 kV being the absolute maximum operating voltage of the capacitor bank. An image of this arc taken by HSC is presented in Fig. 15. As it can be observed, the arc column is not straight, presents tortuosity and does not seem likely to be planar as discussed by Tholin[18]. Considering inter electrode distances from 100 mm to 1.5 m and without referring to the real length of the tortuous electric arc, the mean linear arc resistance can be measured by dividing the mean arc voltage by the regulated current level. The mean value obtained is around 2.5 Ω/m and is in accordance with the experiments results of Sunabe[15].

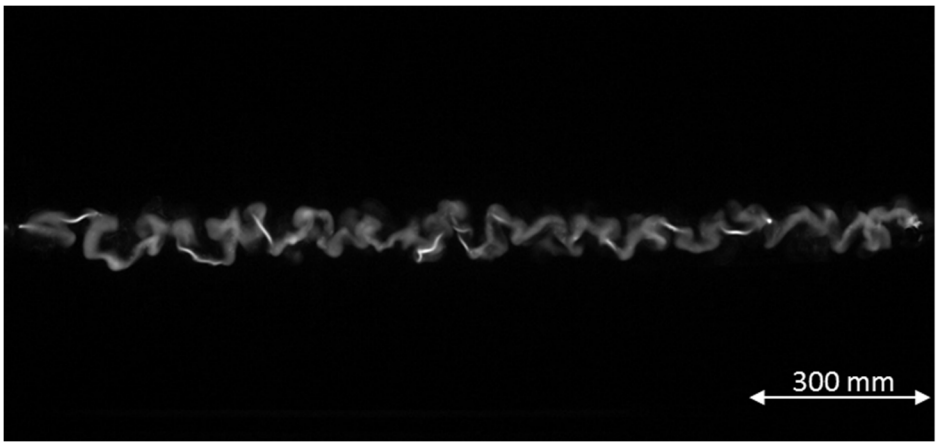

FIG. 15. Image of a C*-waveform electric arc of 1.5 meters

Moreover, to check the robustness of the lightning generator when a restrike phenomenon occurs, tests were conducted using an air blower placed at 50 mm of the arc column. The muzzle velocity of the air was about 60 m/s and its velocity dropped to 25 m/s at 300 mm. the positive electrode - a tungsten rod of 10 mm diameter and 1 meter long – is placed horizontally at 10 cm over the negative electrode - a square aluminum plate of 400 × 400 × 2 mm^3 recovered by a layer of 500 µm dielectric paint. The initial voltage in the capacitor is 2 kV and the current set point is 400 A. The current and voltage waveforms are depicted in Fig. 16.

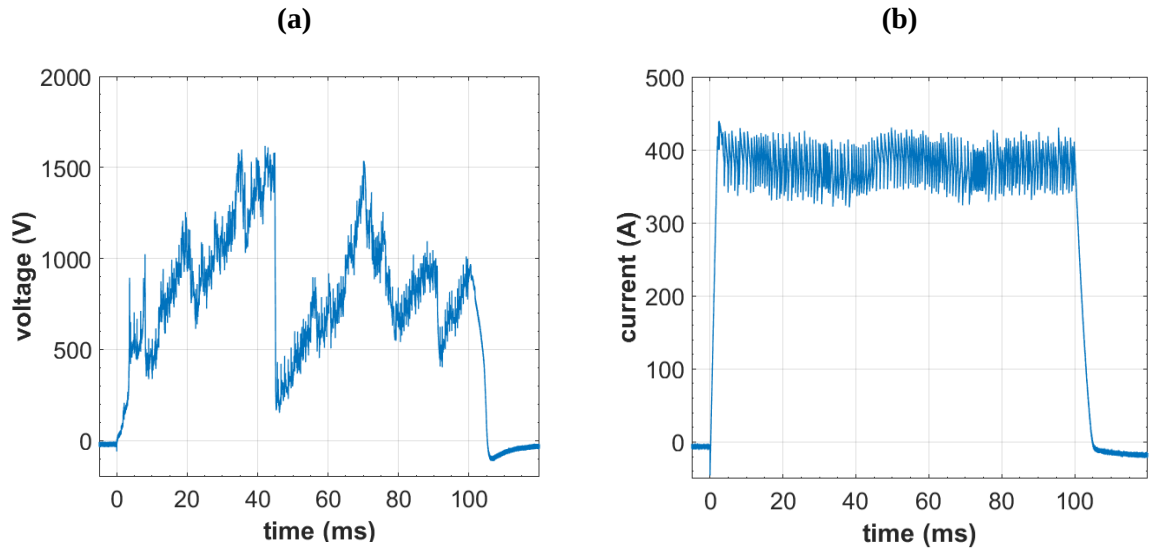

FIG. 16. Voltage (a) and current (b) waveforms of a blown arc

It can be observed in the Fig. 16 that despite the significant drops of arc voltage, especially the one occurring at 45 ms, the current waveform remains stable between its set point values. The arc voltage drop occurring at 45 ms is a result of a restrike, and decreases from 1.6 kV to 200 V in less than 300 µs. A sequence of images of this restrike is presented in Fig. 17.

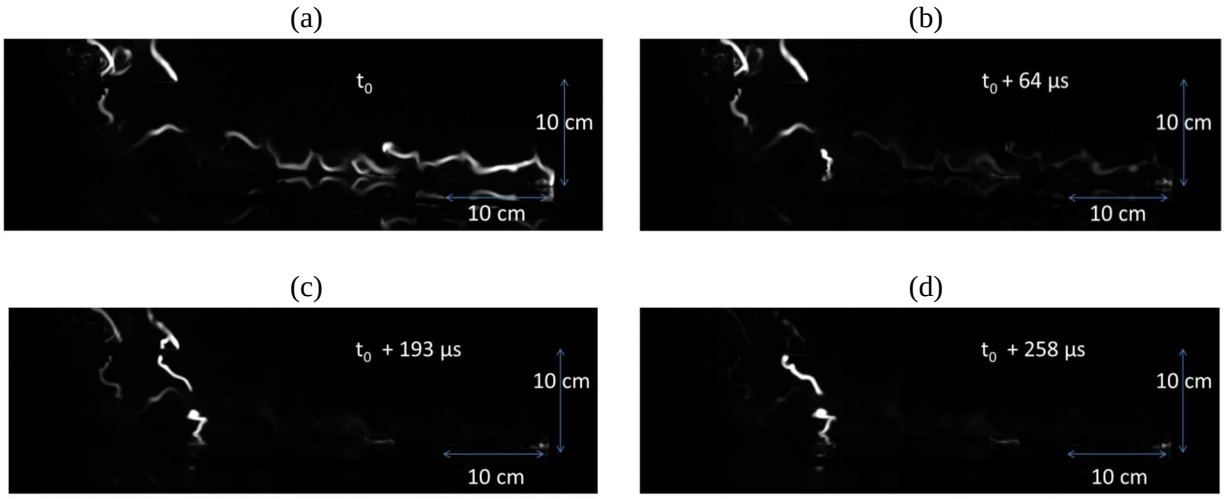

FIG. 17. Sequence of pictures issued from a restrike phenomenon from instant t_0 = 44.904 ms (a) t_0 (b) t_0 + 64 µs (c) t_0 + 193 µs (d) t_0 + 258 µs

It can be observed from the Fig. 17 that the observed phenomenon consists in two consecutive restrikes: one for the square aluminum plate electrode in the bottom electrode from images (a) to (b) from Fig. 17 followed by on for the tungsten rod above electrode from images (c) to (d). For the first restrike, as the layer of dielectric paint recovers the square aluminum plate, no restrike can occur at its surface. Thus the observed restrike occurs because the electric arc crosses the total 400 mm length of the plate and is able to restrike at its other edge which is not protected by the layer. A distance of 400 mm is measured between the two successive arc roots but it is not possible to estimate the real distance of the arc channel that is vanishing during this restrike since just one camera was used. For the second restrike, the arc channel that is vanishing is even partially out of the pictures. Considering that the arc resistance is around 2.5 Ω/m, as measured in the previous part, and that there is a drop of 1.4 kV for a 400 A arc current, 1.4 m of arc column are estimated to have vanished during the two restrikes. Thus, the lightning

generator developed in this work has proved to be able to provide a robust current regulation that enables to overcome the fast length variations of the arc column occurring during restrikes.

V/ Conclusion

A theoretical and experimental study comparing the performances of Buck and Buck-boost topologies as high current generators for lightning arc up to 1 m long and respecting the C* waveform was carried out.

As previous electric simulations of arcs showed that such C*-waveform arcs can be modeled as linear resistors from 2.4 to 8 Ω/m, a comparison of DC/DC converters Buck and Buck-boost topologies and RLC circuit, using a capacitive load as energy source, was conducted considering the lowest level of energy criterion to furnish a C*-waveform through an 8 Ω resistor. Buck topology turned out to require an initial voltage level of 3.5 kV in the capacitor whereas the Buck-boost topology only needed 1.5 kV from a capacitor bank of 100 mF.

The experimental implementations of Buck and Buck-boost topologies have been conducted focusing on the optimization of the feedback loop for the current regulation. The need to find a compromise between the accuracy of the regulation and the respect of the operative electrical parameters of every device of loop has been addressed. Amongst other problems, the transient overvoltage peak occurring at the switching-off of IGBT switch devices – that is likely to break components – is solved by designing a Snubber filter and by reducing the commutation frequency, as well as the reduction of peripheral parasitic inductance coming from the geometry.

With these last optimizations, the Buck and Buck-boost configurations have been experimentally tested and compared with the given performance criteria for a 4 Ω load resistor and for electric arcs from 0.1 to 1.5 m. Whereas the Buck configuration performed a C*-waveform through both the load resistor and electric arcs starting from 100 mm and up to a value of 1.5 m, the Buck-boost configuration turned out to be inefficient to reproduce this waveform for electric arcs. In the other hand, Buck-boost had a best performance for a static resistor of 4 Ω, requiring 1.6 kV against 2 kV for the Buck configuration. This diversion of the Buck-boost experimental performances from the simulations is likely to be caused by the limitation current in the intermediate coil that was implemented to avoid damaging the switching devices. Eventually, the 1.5 m C*-waveform electric arc has been achieved with an initial voltage of 2.3 kV and an equivalent linear resistance of 2.5 Ω/m was experimentally found for 400 A arcs. It proved also to provide an accurate regulation even in case of a restrike phenomenon. For future works, the lightning current generator developed in this work will be used to study and characterize the physical parameters present in the interaction of long lightning arcs with aeronautical materials especially to study the restrike phenomenon.

Acknowledgements

The authors wish to thank the French Civil Aviation Authority (DGAC) for its support.

Data Availability

The data that support the findings of this study are available within the article.

References

[1]B. Fisher, R. Taeuber, and K. Crouch, in *AIAA 26th Aerospace Sciences Meeting, Reno, USA* (1988).

[2]C. Jones, D. Rowse, and G. Odam, in *Int. Conf. on Lightning and Static Electricity, Seattle, USA* (2001).

[3]K. C. Hsu, K. Etemadi, and E. Pfender, J. Phys. D: Appl. Phys. **54**, 1293 (1983).

[4]J. Haidar, J. Phys. D: Appl. Phys. **32** 263 (1999).

[5]F. Lago F., J.J Gonzalez, P. Freton, F. Uhlig, N. Lucius, G.P. Piau, J. Phys. D: Appl. Phys. **39** 2294 (2006).

[6]L. Chemartin, P. Lalande, E. Montreuil, C. Delalondre, B. Chéron, F. Lago, Atmos Res, 91 (2–4) (2009).

[7]L. Chemartin, P. Lalande, C. Delalondre, B. Chéron, F. Lago, J. Phys. D: Appl. Phys. **44** 194003 (2011).

[8]SAE ARP5577 and Eurocae ED-113, *Aircraft Lightning Direct Effects Certification* (AE-2 Lightning Committee, SAE International, London, 2008).

[9]SAE ARP5412B and Eurocae ED-105A, *Aircraft Lightning Environment and Related Test Waveforms* (AE-2 Lightning Committee, SAE International, London 2013).

[10]Eurocae ED-84, *Aircraft Lightning Environment and Related Test Waveforms Standard*, (2013).

[11]S. A. Wutzke, E. Pfender, and E. R. G. Eckert, AIAA Journal, **6** 8, (1968).

[12]F. Tholin, L. Chemartin and P. Lalande, *in Int. Conf. on Lightning and Static Electricity, Toulouse* (2015).

[13]J. A. Dobbing and A. W. Hanson, *in 1978 International Symposium on Electromagnetic compatibility,* Atlanta (1978).

[14]R Sousa Martins, L. Chemartin, C. Zaepffel, P. Lalande and A. Soufiani, *J. Phys. D: Appl. Phys.* **49** 185204 (2016)

[15] P. Leichauer, *Design and development of lightning waveform generators* (PhD. Thesis. Cardiff University. 2017).

[16]B. M. Kovalchuk, A. V. Kharlov, , A. A. Zherlytsyn, E. V. Kumpyak, and N. V. Tsoy, Rev. Sci. Instrum. **87**, 063505 (2016).

[17]M. Caldwell and L. E. Martinez, *in 2005 International Symposium on Electromagnetic Compatibility, Chicago* (2005).

[18]W. Weizel and R. Rompe, Ann. Phys. **436** (1947).

[19]A.E. Vlastos, J. Phys. D: Appl. Phys. **40** 4752-60 (1969).

[20]A.E.Vlastos, J. Appl. Phys. **43** 1987-89 (1972).

[21]K. Sunabe and T. Inaba, I.E.E. Japan Volume 110, Issue 1 (1990).

[22]L. Chemartin, *Modélisation des arcs électriques dans le contexte du Foudroiement des aéronefs* (PhD. Thesis. Université de Rouen. 2008).

[23]D. A. Garren and J. Chen, Phys. Plamas 1, 3425 (1994).

[24]S. Tanaka S, K. Sunabe, and Y. Goda, *in 13th Int. Conf. on Gas Discharges and their applications, Glasgow* (2000).

[25]Y. Fuad, W.L. de Koning, J.W. van der Woude, IJEEE **38**.1.5 (2001).

[26]Y. Yamashita, J. Furuta, S. Inamori and K. Kobayashi, *in 18th Workshop on Control and Modeling for Power Electronics*, Stanford (2017).

[27] X. Li, Y. Luo, Y. Duan, B. Liu, Y. Huang and F. Sun, *2018 IEEE International Power Electronics and Application Conference and Exposition (PEAC)*, 2018

[28]A. Algaddafi and K. Elnaddab, *in 4th International Renewable and Sustainable Energy Conference*, Marrakech (2016).

[29]R. Severns and E. Reduce, *Design of snubbers for power circuits*, (*International Rectifier Corporation*, 2009).

[30]A. Kadivar, K. Niayesh, N. Støa-Aanensen and F. Abid, J. Phys. D: Appl. Phys. **54** 055203. (2020)